Water-Soluble Palladium Nanoclusters Catalysts in Ligand-Free Suzuki-Miyaura Cross-Coupling Reactions

Priya Karna[†], Micheal Okeke[†], Debora Motta Meira^{γ,||}, Zou Finfrock^{γ,||}, and Dong-Sheng Yang^{†,*}

[†]Department of Chemistry, University of Kentucky, Lexington, KY 40506, USA

⁷CLS@APS sector 20, Advanced Photon Source, Argonne National Laboratory, 9700 S. Cass Avenue, Argonne, IL 60439, USA

Canadian Light Source Inc., 44 Innovation Boulevard, Saskatoon, Saskatchewan S7N 2V3, Canada

KEYWORDS: cross-coupling, homogeneous catalysis, palladium nanoclusters, Pd(II) reduction, UV/Vis spectroscopy, photoelectron spectroscopy, x-ray absorption spectroscopy.

Supporting Information Placeholder

ABSTRACT: This letter reports Pd-nanocluster catalysts and their formation in ligand-free Suzuki-Miyaura reactions with Pd(II) nitrate as a precatalyst. The catalysts are water-soluble neutral Pd tetramer and trimer in their singlet electronic states as identified by UV-Vis absorption spectroscopy and are formed by leaching of spherical Pd(0) nanoparticles with an average diameter of about three nanometers. The Pd(0) nanoparticles are produced by reducing Pd(II) nitrate and characterized with transmission electron microscopy and Pd-K edge extended x-ray fine structure spectroscopy. The Pd(II) reduction is induced by ethanol and enhanced by potassium hydroxide and monitored with x-ray photoelectron spectroscopy.

Transition-metal catalyzed cross coupling is a powerful synthetic method for constructing carbon-carbon and carbon-heteroatom bonds in pharmaceuticals, agrichemicals, and precursors for materials. ¹⁻⁶ Among various cross-coupling schemes, the Suzuki-Miyaura (SM) reaction uses an organoboron nucleophile and an organic halide electrophile as coupling partners and has the most important technical significance due to the relatively mild reaction conditions and the non-toxic, air/moisture tolerant nature, and wide availability of organoboron derivatives. ⁵, ⁷⁻⁸ Although ligand-stabilized, unsaturated Pd(0) complexes are generally known as catalysts in solution-phase cross-coupling reactions, new catalytical species have recently been proposed for both homo- and hetero-geneous reactions. ⁹⁻¹³

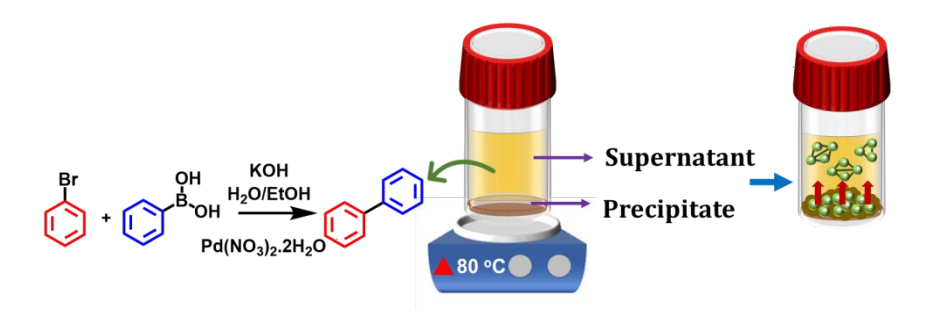
For reactions employing Pd complexes that are stabilized with phosphine ligands, unusual Pd(I) and Pd₃(IV) catalysts were reported recently.⁹⁻¹¹ The Pd(I) catalyst was a binuclear complex and formed by the reduction of a Pd(II) precursor in the presence of a phosphine ligand.⁹ The formation of the Pd(I) species depended on the nature of the Pd (II) precursor, the choice of the phosphine ligand, the stoichiometry of the Pd to phosphine, and the order of the addition of the reagents. The Pd₃(IV) catalyst with each Pd atom in an oxidation state of +4/3 was formed by the reaction

of a Pd(II) salt and a phosphine in the presence of NaBH₄.¹⁰ In the SM coupling between various aryl bromides and phenylboronic acid, the Pd₃(IV) catalyst reacted first with phenylboronic acid to generate an intermediate, which is in contrast to the well-established SM coupling mechanism where an oxidative addition is the first step.¹⁰ As to the transmetallation step, tri- and tetra-coordinate boron complexes were identified as containing Pd-O-B linkages.¹⁴

For ligand-free cross-coupling reactions with Pd-containing solids, the physical state and chemical identity of catalytical species remains under debate.5,12-13, 15-21 Several studies proposed that Pd catalysts were in solid states, ^{12-13, 15, 22} while others argued that they were molecular species produced by leaching of solid precatalysts in solutions. 16-21 In supporting the argument of heterogeneous catalysis, a stable single-atom Pd catalyst anchored on exfoliated graphitic carbon nitride was reported through scanning transmission electron spectroscopy; 12 a direct contact between aryl bromides with the metal surface of Au-Pd superstructures was proposed through surface-enhanced Raman spectroscopic measurements; 13 and the SM coupling reactivity was observed to correlate with surface changes on Pd nanoparticles supported on carbon nanotubes. 15 On the other hand, there is emerging evidence toward a scenario that Pd-containing solids only serve as a reservoir of soluble catalytically active Pd species. 16 However, the chemical identity of the soluble Pd species is being actively debated. Several studies proposed Pd oxides as active species leached out from Pd supported on metal oxides, nanotubes, wire, foil, or sponge, 16-17, 19 while others suggested small Pd clusters formed in N-methyl pyrrolidone as active species, 18 or the identity of the molecular species in solutions was unknown.²⁰⁻²¹

60

Scheme 1. Water-soluble $Pd_{3,4}$ nanoclusters formed by leaching of Pd (0) nanoparticles catalyze the SM coupling between C_6H_5B and $C_6H_5B(OH)_2$ with $Pd(NO_3)_2.2H_2O$ as a precatalyst.



In this work, we have identified water-soluble neutral Pd₄ and Pd₃ nanoclusters as catalysts in the SM coupling reaction between bromobenzene and phenylboronic acid with Pd(II) nitrate as a precatalyst and in the presence of ethanol and potassium hydroxide (Scheme 1). The Pd_{4,3} nanoclusters are formed by leaching of spherical Pd(0) nanoparticles in the reaction medium. The Pd(0) nanoparticles are produced by the reduction of Pd(II) nitrate, and the reduction is induced by the alcohol and enhanced by the base.

To investigate if the SM coupling is catalyzed homogeneously or heterogeneously, we performed the reactions separately with water-soluble Pd species and solid Pd particles. The soluble and solid Pd were isolated from catalytical mixtures that were prepared at 80 °C in two batches: one with the bromobenzene and phenylboronic acid substrates (batch A) and the other without them (batch B), both in the presence of Pd(II) nitrate, potassium hydroxide, water, and ethanol. Upon isolation, the soluble Pd species reside in the inorganic layer of the supernatant while the solid Pd particles are in precipitate. The SM reactions were then carried out at 80 °C, separately with the inorganic supernatants and precipitates isolated from the two batch mixtures in fresh base and alcohol aqueous solutions. The details of the mixture preparation, isolation, and SM reactions are presented in Figures S1 and S2, and results are summarized in Table 1. The yields of the coupling product, biphenyl, were measured by gas chromatography-mass spectrometry (GC-MS) (Figures S3-S5). As shown in the table, both the soluble and solid Pd prepared from batch A exhibit a high catalytical activity, while with batch B, only the soluble Pd species catalyzes the SM reaction.

Table 1. SM coupling of bromobenzene and phenylboronic acid substrates catalyzed by soluble Pd species and solid Pd particles isolated from catalytical mixtures.

Mixturea		()	rith Pd	Yield (%) solid particles ^b	with Pd
With (batch A)	substrates	91		89	
Without (batch B)	substrates	61		0	

 $^{^{}a}$ In both cases, the mixtures consisted of Pd(NO₃)₂.H₂O (0.0375 mmol), KOH (0.96 mmol) and 4 mL 1:1 H₂O: CH₃CH₂OH and were stirred in air at 80°C for 0.5 h (batch A) and 1 h (batch B).

To help understand the activity difference between the solid Pd from the two mixtures, we measured the Pd 3d x-ray photoelectron spectra (XPS) and observed the Pd particles prepared from the two batches are both in the zero-oxidation state even though their reaction yields are 0 and 89%, respectively. We also measured UV-Vis spectra of the inorganic layers isolated from the reaction mixtures and found that the spectra are the same with the soluble and solid Pd prepared with the substrates. These spectroscopic measurements suggest that the Pd(0) particles themselves are not an active catalyst but serves as a reservoir from which catalytical species are discharged into the solutions, which is consistent with numerous previous studies. 16-21 The leaching and activity are enhanced for the solid Pd (0) particles that were isolated from the mixture with the organic substrates, as previously reported for Pd supported on alumina or carbon in SM and Heck reactions.²³⁻²⁴ Activity enhancement is also observed for the soluble Pd species from the mixture with the substrates. In addition, we tested the activity of the soluble and solid Pd from the two batch mixtures prepared at the room temperature and found that the reaction yields (e.g., 83 and 66% for the soluble and solid Pd, respectively, with the substrates and no product for both Pd without the substrates) are lower than those prepared at 80 °C (Table 1) This observation suggests that an increased temperature enhances the Pd leaching and activity as well.

We then investigated the reusability and stability of the watersoluble Pd catalyst. Figure 1 presents the yields of biphenyl obtained from several runs by using the soluble and solid Pd isolated from the mixture with the substrates, each run was carried out in triplicate. The yields of biphenyl from the first three consecutive runs were similar in two cases. After the third run, the reaction with the Pd(0) particles delivered no product, while the reaction with the soluble Pd species still showed fair activity in two additional runs under the same conditions. The fewer catalytical cycles with the Pd (0) particles are likely due to the redeposition of the discharged soluble Pd species on the surface of the solid. To test the stability of the soluble Pd species in the solution, we performed the SM coupling after the fresh inorganic supernatant was stored at room temperature for 12 weeks and found the reaction generated biphenyl with 40% yield. This observation shows the water-soluble Pd species is very stable under ambient conditions, a clearly desirable property for any catalysts.

^b Yields of biphenyl were measured with GC-MS. SM coupling reactions of bromobenzene and phenylboronic acid were carried out with stir in air at 80°C for 0.5 h (with batch A) or 1 h (with batch B) in the solution of KOH (0.96 mmol) and 4 mL 1:1 H₂O: CH₃CH₂OH.

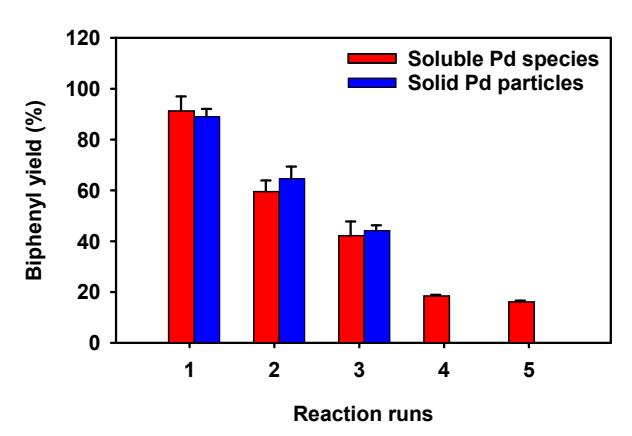


Figure 1. Comparison of biphenyl yields of the SM reaction catalyzed with soluble Pd species (red) and Pd(0) particles (blue). The yields were measured with GC-MS.

To confirm that biphenyl was formed by the SM cross-coupling between C_6H_5Br and $C_6H_5B(OH)_2$, rather than through the homocoupling of C_6H_5Br or $C_6H_5B(OH)_2$, we carried out three control experiments with a) $C_6H_5B(OH)_2$, we carried out three control experiments with a) $C_6H_5B(OH)_2$, and c) 2-bromotoulene (C_7H_7Br) and $C_6H_5B(OH)_2$. These reactions were conducted separately with the soluble Pd species from the mixtures with and without substrates. The reactions with only C_6H_5Br or $C_6H_5B(OH)_2$ yielded no product in both cases, whereas the cross coupling of C_7H_7Br and $C_6H_5B(OH)_2$ produced the product of 2-phenyltoleuene in 90% yield with the substates and 53 % without them (Scheme S1 and Figures S6 ad S7).

After the identification of the SM coupling being catalyzed by water-soluble Pd species, we proceeded with the experiment to determine their chemical identities. It is observed that the soluble Pd species consist of Pd_4 as the major species and Pd_3 as the minor one, as shown by comparing the experimental and computational UV-Vis spectra in Figure 2. The experimental spectrum was obtained by subtracting the spectrum of the spent inorganic supernatant after the final run from the spectrum of a fresh solution prior to the SM reaction to minimize the interference from organic chemicals. The supernatant after the final run contains no Pd clusters, while the clusters are not consumed in the fresh solution. The experimental spectrum was recorded in the range of 200-700 nm, but no signal was observed beyond 400 nm. The theoretical spectra were computed using

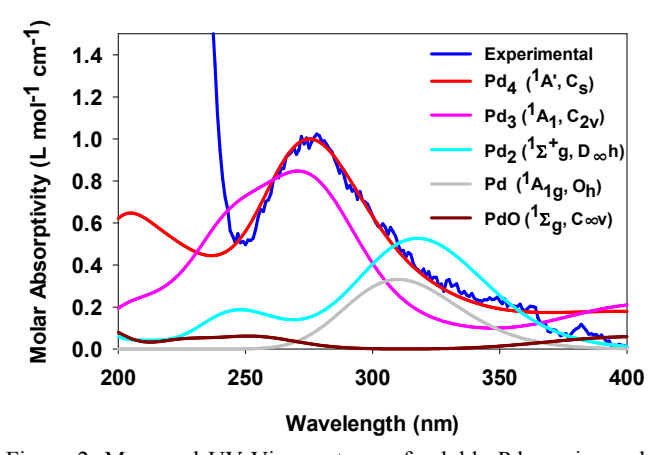
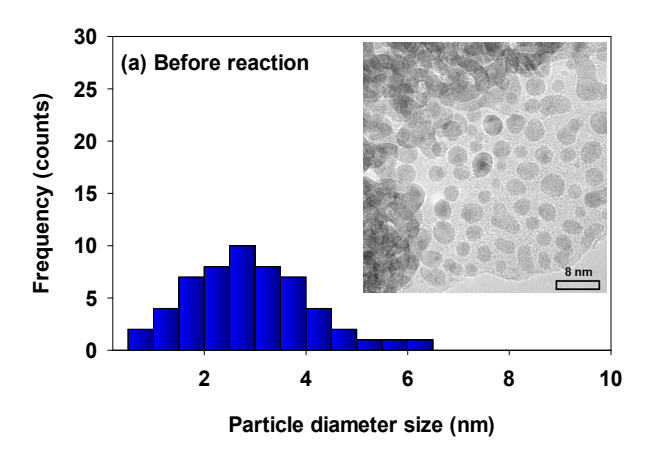


Figure 2. Measured UV-Vis spectrum of soluble Pd species and calculated spectra of Pd_{1-4} and PdO by TD-DFT calculations with the continuum solvation model.

Time-dependent density functional theory (TD-DFT), and the solvent (i.e., water) effect was treated by the polarizable continuum model.²⁵ We considered several small Pd_n species (n=1-4) and PdO in our calculations because these two classes of molecules were previously proposed as possible catalytical species in ligand-free Pd-catalyzed SM reactions. 16-19 Because they are stable in aqueous solutions under ambient atmosphere, these species are expected to be in singlet electronic states where all electrons are paired, rather than other spin states with one or more unpaired electrons. The singlet spin states are the electronic states of the neutral molecules. The calculated spectrum of a nearly-planar Pd₄ cluster (¹A', C₈) shows well-matched maximum absorption wavelength (~ 275 nm) and profile with the measured spectrum. The spectrum of a planar Pd₃ cluster (¹A₁, C_{2v}) displays a much broader absorption profile and a lower intensity with the maximum at ~ 270 nm. Its contribution may not be excluded but must be considerably smaller than that of the Pd₄ cluster. For other species, the spectral maxima are predicted at 309 nm for Pd (1 S), 316 nm for Pd₂ ($^{1}\Sigma_{g}^{+}$, $D_{\infty h}$) and 250 nm for PdO (${}^{1}\Sigma^{+}$, $C_{\infty \nu}$); all have much lower intensities. Thus, these molecules are not significant in the supernatant. The Pd tetramer and trimer (Figure S8) serve as a catalyst because they are the major soluble Pd species, their existence leads to the formation of the coupling product, and they are the reactants and products in multiple runs until their activity is diminished. The current work is consistent with the previous study where Pd_{3.4} clusters formed in N-methylpyrrolidone and estimated with the jellium model were proposed to be active species, 18 but inconsistent with other studies where palladium oxides were reported to be catalytically active. 16-^{17, 19} However, the electronic states and relative contributions of the Pd clusters were not identified with the jellium model that was used for size estimation in the previous study. 18 Nevertheless, it is interesting that the jellium model that is based on the uniform electron gas and often used in solid physics is capable for estimating the size of such small metal clusters in aqueous solutions. We have also located a singlet Pd₄ cluster in a three-dimensional structure. However, the calculated UV-Vis spectrum of the threedimensional Pd₄ singlet state has a much lower intensity and broader absorption than that of the experimental spectrum (Figure S9). Thus, the three-dimensional Pd₄ is not a significant species of the catalyst.

The next issue that was addressed is the size and shape of the solid Pd particles that serves as the reservoir of the Pd clusters. Figure 3 shows the transmission electron microscopy (TEM) images of the Pd nanoparticles prior to the SM reaction (a) and after the final run (b), taken with the electron beam perpendicular to the sample surface, while those in Figure S10 are images taken at other angles. Before the SM reaction, most of the Pd nanoparticles have a spherical shape, and the average diameter of fifty-five nanoparticles is estimated to be 2.99 ± 1.32 nm. After the final run of the SM reaction, the shape of most Pd nanoparticles becomes roughly cylindrical with the average dimension of 2.71 \pm 1.18 nm in diameter and 7.42 ± 0.97 nm in length. The spherical shape of the Pd nanoparticles before the reaction suggests that the constituent molecular species have negligible total electric dipole moments. Indeed, the electric dipole moments of the Pd₄ and Pd₃ clusters are predicted to be zero and 0.027 D, respectively. On the other hand, the cylindrical shape of the Pd nanoparticles after the final run of the reaction suggests that the constituent inactive molecular species should have a larger electric dipole in one direction than those in other two directions. One of the inactive species is presumably PdO, which is predicted to have the electric dipole of 8.352 D along the molecular axis and zero along the axes perpendicular to the molecular axis.



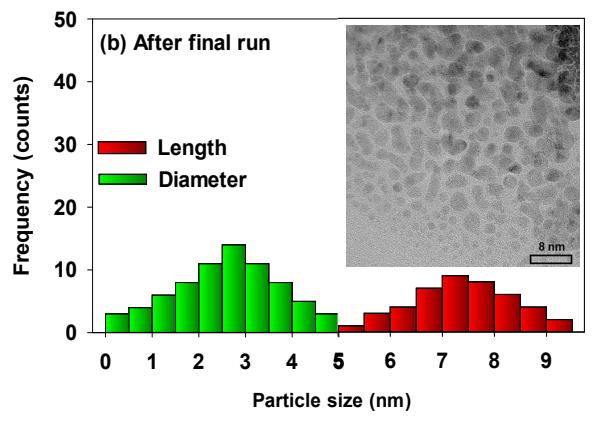


Figure 3. TEM images and size histograms of the spherical Pd nanoparticles before the SM reaction (a) and the cylindrical Pd particles after the final run (b). The dimension of the cylindrical particle size is represented by the diameter of the cross section and the length.

The existence of PdO on the surface of the Pd nanoparticles after the final run of the reaction is also consistent with the XPS measurements, where Pd(II) was observed as a major oxidation state (Figure S11). In contrast, only Pd(0) was detected on the surface of the Pd nanoparticles before the reaction (Figure S11). To investigate the local coordination of the Pd nanoparticles, we Pd-K-edge x-ray absorption performed spectroscopic measurements. The extended x-ray absorption fine structure (EXAFS) single-shell fits in the R-space indicate that the local coordination number of Pd-Pd is 4.3 ± 0.9 for the sample before the reaction and reduces slightly to 3.4 ± 0.6 for the sample after the final run of the reaction (Table 2 and Figure S12). The EXAFS measurements are consistent with the UV-Vis spectra that show the Pd_{4.3} clusters are leached to the supernatant from the surface. The EXAFS measurements also show an increase of Pd-O from the before-reaction to the after final-run sample. Such an increase correlates with the degradation of activity of the Pd catalyst.

Table 2. EXAFS parameters from the best single-shell fits.^a

	N _{Pd-O}	R _{Pd-O} (Å)	N _{Pd-Pd}	R _{Pd-Pd} (Å)	$\sigma_i^2 (\mathring{A}^2)$
Pd foil			12	2.740 (2)	0.0054(4)
Pd(NO ₃) ₂	2	2.02 (2)			
Sample 1	1.1(4)	1.97 (4)	4.3 (9)	2.75 (1)	0.009(1)
Sample 2	1.7(3)	1.99 (2)	3.4 (6)	2.78 (1)	

^aFor Pd(NO₃)₂, only the first Pd-O contribution is listed in the table.

Sample 1: the sample before the reaction.

Sample 2: the sample after the final run of the reactions.

$$\begin{array}{l} \Delta E_{0(Pd\text{-Pd})} = 0.8 \pm 1; \; S_0{}^2_{(Pd\text{-Pd})} = 0.78 \pm 0.04; \; S_0{}^2_{(O\text{-O})} = 1.1 \pm 0.2; \\ \Delta E_{0(Pd\text{-O})} = 8 \pm 2; \; \Delta E_{0(Pd\text{-foil})} = 4.6 \pm 0.3 \end{array}$$

The Pd(0) nanoparticles are formed by the reduction of Pd(II) nitrate induced by ethanol and enhanced by potassium hydroxide at the room and reaction (80 °C) temperatures. The reduction was monitored by the XPS measurements of Pd 3d electron binding energies (Figure 4). For Pd(NO₃)₂.2H₂O dissolved in water (Figure 4a), the Pd (II) 3d electron binding energies are measured to be 337.2 and 342.5 eV, which correspond to the $3d_{5/2}$ and $3d_{3/2}$ spinorbit terms, respectively. The energy ordering of the two spin-orbit terms arising from the 3d⁹ configuration upon ionization is consistent with Hund's rules, where for a more than half-filled subshell, the state with a larger total angular momentum J has a lower binding energy. The relative intensity of the $3d_{5/2}$ to $3d_{3/2}$ bands is governed by the (2J+1) degeneracy of each term, where J = 5/2 and 3/2. There is a weak satellite band at the higher energy side of each main band, and these weak bands arise from a shakeup process where the outgoing 3d electron interacts with a valence electron and excite it to a higher energy level. The addition of KOH to the Pd(II) nitrate solution has no effect on the Pd 3d binding energies (Figure 4b), implying that the Pd oxidation state remains to be +2. However, the addition of ethanol to the Pd(II) nitrate solution produces two extra bands in the XPS spectrum (Figure 4c), and these two bands are easily assigned to Pd(0) $3d_{5/2}$ at 335.2 eV and 3d_{3/2} at 340.5 eV. Surprisingly, adding KOH to the solution of Pd(II) nitrate and ethanol vanishes the Pd(II) 3d bands (Figure 4d), indicating that the reduction of Pd(II) to Pd(0) is now complete. We also measured the Pd 3d photoelectron spectra for the soluble Pd species by using an increased amount of Pd(II) nitrate to obtain a reasonable XPS signal. We observed that Pd in the supernatant is in zero-oxidation state (Figure 4e), which is consistent with the comparison of the experimental and computed UV-Vis spectra that shows Pd_{4,3} are neutral clusters. The slightly blue shift of the Pd 3d electron binding energy (0.4 eV) from the nanoparticles in the precipitate to the soluble species in the supernatant reflects the well-known size-dependent electron property of metal clusters and particles.26

The comparison of the Pd 3d photoelectron spectra in Figure 4(a-d) shows that ethanol acts as the reducing agent for the reduction of $Pd(NO_3)_2.2H_2O$ and KOH enhances the alcohol-induced reduction even though the base alone is not capable to reduce the palladium salt. These observations can be understood by the following two reactions:

$$CH_3CH_2OH + Pd(NO_3)_2 = Pd(0) + CH_3CHO + 2HNO_3$$
 (1)

$$KOH + HNO_3 = KNO_3 + H_2O$$
 (2)

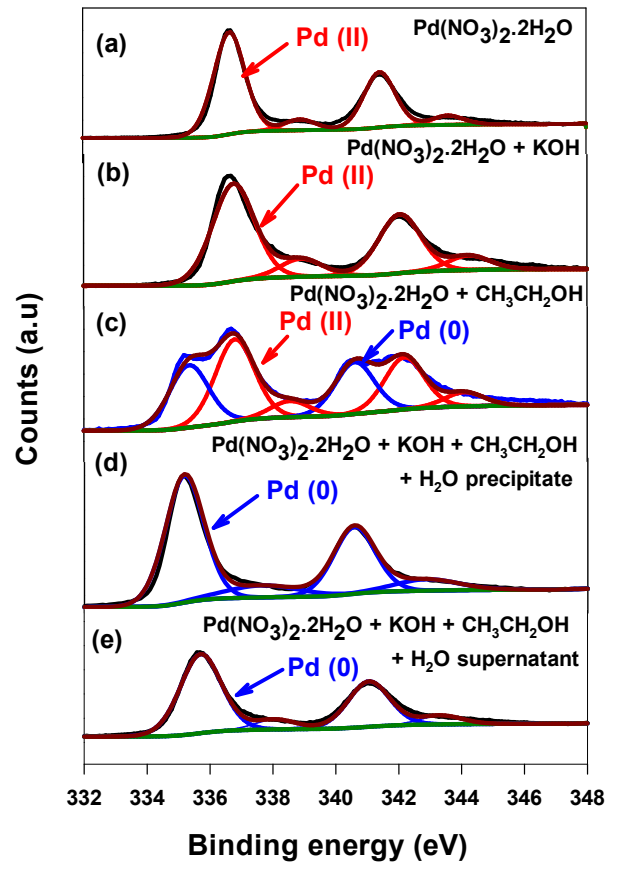


Figure 4. XPS spectra of Pd 3d for the aqueous solutions of Pd(NO₃)₂.2H₂O (a), Pd(NO₃)₂.2H₂O + KOH (b), Pd(NO₃)₂.2H₂O + CH₃CH₂OH (c), and Pd(NO₃)₂.2H₂O + CH₃CH₂OH + KOH [(d) for the precipitate and (e) for the supernatant].

The observed ethanol-induced Pd(II) reduction (1) is consistent with well-known Pd-catalyzed oxidation of alcohols.²⁷ The formation of CH₃CHO is confirmed by the ¹³C NMR spectrum in Figure S13, where the 30.7 and 200.83 ppm bands are indicative of the production of acetaldehyde.²⁸ The Pd(II) reduction is enhanced by the simple acid-base reaction (2), which consumes nitric acid and thus shifts the reduction equilibrium to the Pd(0) side. The role of the base observed in this work is complementary to the previously reported base effect on the transmetallation and reductive elimination in Pd-catalyzed SM reactions.²⁹⁻³⁰

In summary, we report Pd-nanocluster catalysts and their formation in the SM coupling reaction between benzene bromide and phenylboronic acid with palladium nitrate as a precatalyst. The SM coupling is homogenous in nature without any stabilizing organic ligands. The Pd catalyst consists of mainly neutral Pd tetramers with sescondary Pd trimers in their singlet electronic states. The Pd nanoclusters are generated by leaching of the Pd(0) nanoparticles and stable in aqueous solutions for at least three months at the room temperature. The Pd(0) nanoparticles are formed by reducing Pd(II) nitrate, and the reduction is induced by ethanol and enhanced by potassium hydroxide. Without the base,

the extent of the Pd(II) nitrate reduction is not sufficient for the SM coupling. Although this study is carried out with Pd(II) nitrate as a precatalyst and ethanol and potassium hydroxide as reducing agents, we envision that conclusions reached in this work about the Pd catalyst will likely be valid for SM reactions with other inorganic Pd(II) salts as precatalysts and other alcohols and bases as Pd(II) reducing agents.

ASSOCIATED CONTENT

Supporting Information

The Supporting Information is available free of charge. Experimental and computational details, reaction scheme of the control experiment (Scheme 1), flowchart of reaction protocols (Figures S1 and S2), GC-MS calibration curve of pure biphenyl (Figures S3), GC-MS spectra of the organic layers from C₆H₅Br and C₆H₅B(OH)₂ coupling reaction (Figures S4 and S5), GC-MS calibration curve of pure 2-phenyltoluene (Figure S6), GC-MS spectra of the organic layer from the C₇H₇Br and C₆H₅B(OH)₂ coupling reaction (Figure S7), structures of the Pd nanoclusters (Figure S8), experimental UV-Vis spectra of the soluble Pd species and the TD-DFT calculated spectrum of a three-dimensional Pd₄ nanocluster in the singlet electronic state (Figure S9), TEM images of the Pd nanoparticles at different angles (Figure S10), Pd 3d XPS spectra of Pd nanoparticles (Figure S11), Pd K-edge EXAFS single-shell fits in R-space of Pd nanoparticles (Figure S12), and ¹³C NMR spectrum of the organic-layer reaction mixture formed by the Pd(NO₃)₂.2H₂O reduction with ethanol and potassium hydroxide.

AUTHOR INFORMATION

Corresponding Author

Dong-Sheng Yang - Department of Chemistry, University of Kentucky, Lexington, KY 40506, USA.

Orcid.org/0000-0001-9842-4343.

Email: dyang0@uky.edu (D-S.Y.).

Authors

Priya Karna - Department of Chemistry, University of Kentucky, Lexington, KY 40506, USA.

Micheal Okeke - Department of Chemistry, University of Kentucky, Lexington, KY 40506, USA.

Debora Motta Meira - CLS@APS sector 20, Advanced Photon Source, Argonne National Laboratory, 9700 S. Cass Avenue, Argonne, IL 60439, USA. Canadian Light Source Inc., 44 Innovation Boulevard, Saskatoon, Saskatchewan S7N 2V3, Canada.

Zou Finfrock - CLS@APS sector 20, Advanced Photon Source, Argonne National Laboratory, 9700 S. Cass Avenue, Argonne, IL 60439, USA. Canadian Light Source Inc., 44 Innovation Boulevard, Saskatoon, Saskatchewan S7N 2V3, Canada.

Notes

The authors declare no competing financial interests.

ACKNOWLEDGMENT

We acknowledge financial support from the National Science Foundation Division of Chemistry (Chemical Structure, Dynamics, and Mechanisms, Grant No. 1800316). This research used resources of the Advanced Photon Source, an Office of Science User Facility operated for the U.S. Department of Energy (DOE) Office of Science by Argonne National Laboratory and was supported by the U.S. DOE under Contract No. DE-AC02-06CH11357, and the Canadian Light Source and its funding partners. The authors would also like to thank Dali Qian and Jillian Cramer for their help with TEM.

REFERENCES

- 1. Hazari, N.; Melvin, P. R.; Beromi, M. M., Well-defined nickel and palladium precatalysts for cross-coupling. *Nat. Rev. Chem.* **2017**, *1* (3).
- 2. Devendar, P.; Qu, R. Y.; Kang, W. M.; He, B.; Yang, G. F., Palladium-Catalyzed Cross-Coupling Reactions: A Powerful Tool for the Synthesis of Agrochemicals. *J. Agric. Food Chem.* **2018**, *66* (34), 8914-8934.
- 3. Choi, J.; Fu, G. C., Transition metal-catalyzed alkyl-alkyl bond formation: Another dimension in cross-coupling chemistry. *Science* **2017**, *356* (6334), eaaf7230
- 4. Campeau, L.-C.; Hazari, N., Cross-Coupling and Related Reactions: Connecting Past Success to the Development of New Reactions for the Future. *Organometallics* **2019**, *38* (1), 3-35.
- 5. Biffis, A.; Centomo, P.; Del Zotto, A.; Zeccal, M., Pd Metal Catalysts for Cross-Couplings and Related Reactions in the 21st Century: A Critical Review. *Chem. Rev.* **2018**, *118* (4), 2249-2295.
- 6. Uehling, M. R.; King, R. P.; Krska, S. W.; Cernak, T.; Buchwald, S. L., Pharmaceutical diversification via palladium oxidative addition complexes. *Science* **2019**, *363* (6425), 405-408.
- 7. Hooshmand, S. E.; Heidari, B.; Sedghi, R.; Varma, R. S., Recent advances in the Suzuki-Miyaura cross-coupling reaction using efficient catalysts in eco-friendly media. *Green Chem.* **2019**, *21* (3), 381-405.
- 8. Miyaura, N.; Suzuki, A., Palladium-Catalyzed Cross-Coupling Reactions of Organoboron Compounds. *Chem. Rev.* **1995**, *95* (7), 2457-2483.
- 9. Johansson Seechurn, C. C. C.; Sperger, T.; Scrase, T. G.; Schoenebeck, F.; Colacot, T. J., Understanding the Unusual Reduction Mechanism of Pd(II) to Pd(I): Uncovering Hidden Species and Implications in Catalytic Cross-Coupling Reactions. *J. Am. Chem. Soc.* **2017**, *139* (14), 5194-5200.
- 10. Fu, F. Y.; Xiang, J.; Cheng, H.; Cheng, L. J.; Chong, H. B.; Wang, S. X.; Li, P.; Wei, S. Q.; Zhu, M. Z.; Li, Y. D., A Robust and Efficient Pd₃ Cluster Catalyst for the Suzuki Reaction and Its Odd Mechanism. *ACS Catal.* **2017**, *7* (3), 1860-1867.
- 11. Proutiere, F.; Aufiero, M.; Schoenebeck, F., Reactivity and Stability of Dinuclear Pd(I) Complexes: Studies on the Active Catalytic Species, Insights into Precatalyst Activation and Deactivation, and Application in Highly Selective Cross-Coupling Reactions. *J. Am. Chem. Soc.* **2012**, *134* (1), 606-612.
- 12. Chen, Z.; Vorobyeva, E.; Mitchell, S.; Fako, E.; Ortuño, M. A.; López, N.; Collins, S. M.; Midgley, P. A.; Richard, S.; Vilé, G.; Pérez-Ramírez, J., A heterogeneous single-atom palladium catalyst surpassing homogeneous systems for Suzuki coupling. *Nat. Nanotechnol.* **2018**, *13* (8), 702-707.
- 13. Zhao, Y.; Du, L.; Li, H.; Xie, W.; Chen, J., Is the Suzuki–Miyaura Cross-Coupling Reaction in the Presence of Pd Nanoparticles Heterogeneously or Homogeneously Catalyzed? An Interfacial

- Surface-Enhanced Raman Spectroscopy Study. *J. Phys. Chem. Lett.* **2019**, *10* (6), 1286-1291.
- 14. Thomas, A. A.; Denmark, S. E., Pre-transmetalation intermediates in the Suzuki-Miyaura reaction revealed: The missing link. *Science* **2016**, *352* (6283), 329-332.
- 15. Shao, L.; Zhang, B.; Zhang, W.; Hong, S. Y.; Schlögl, R.; Su, D. S., The role of palladium dynamics in the surface catalysis of coupling reactions. *Angew. Chem. Int. Ed.* **2013**, *52* (7), 2114-2117.
- 16. Del Zotto, A.; Zuccaccia, D., Metallic palladium, PdO, and palladium supported on metal oxides for the Suzuki-Miyaura cross-coupling reaction: a unified view of the process of formation of the catalytically active species in solution. *Catal. Sci. Technol.* **2017**, *7* (18), 3934-3951.
- 17. Elias, W. C.; Signori, A. M.; Zaramello, L.; Albuquerque, B. L.; de Oliveira, D. C.; Domingos, J. B., Mechanism of a Suzuki-Type Homocoupling Reaction Catalyzed by Palladium Nanocubes. *ACS Catal.* **2017**, *7* (2), 1462-1469.
- 18. Leyva-Pérez, A.; Oliver-Meseguer, J.; Rubio-Marqués, P.; Corma, A., Water-Stabilized Three- and Four-Atom Palladium Clusters as Highly Active Catalytic Species in Ligand-Free C-C Cross-Coupling Reactions. *Angew. Chem. Int. Ed.* **2013**, *52* (44), 11554-11559
- 19. Amoroso, F.; Cersosimo, U.; Del Zotto, A., Studies on the catalytic ability of palladium wire, foil and sponge in the Suzuki–Miyaura cross-coupling. *Inorganica Chim. Acta* **2011**, *375* (1), 256-262
- 20. MacQuarrie, S.; Horton, J. H.; Barnes, J.; McEleney, K.; Loock, H. P.; Crudden, C. M., Visual observation of redistribution and dissolution of Palladium during the Suzuki–Miyaura Reaction. *Angew. Chem., Int. Ed.* **2008**, *47* (17), 3279-3282.
- 21. Thathagar, M. B.; ten Elshof, J. E.; Rothenberg, G., Pd nanoclusters in C-C coupling reactions: Proof of leaching. *Angew. Chem. Int. Ed.* **2006**, *45* (18), 2886-2890.
- 22. Ye, T.-N.; Lu, Y.; Xiao, Z.; Li, J.; Nakao, T.; Abe, H.; Niwa, Y.; Kitano, M.; Tada, T.; Hosono, H. J. N. c., Palladium-bearing intermetallic electride as an efficient and stable catalyst for Suzuki cross-coupling reactions. *Nat. Commun.* **2019**, *10* (1), 1-10.
- 23. Soomro, S. S.; Ansari, F. L.; Chatziapostolou, K.; Kohler, K., Palladium leaching dependent on reaction parameters in Suzuki-Miyaura coupling reactions catalyzed by palladium supported on alumina under mild reaction conditions. *J. Catal.* **2010**, *273* (2), 138-146.
- 24. Gnad, C.; Abram, A.; Urstöger, A.; Weigl, F.; Schuster, M.; Köhler, K., Leaching Mechanism of Different Palladium Surface Species in Heck Reactions of Aryl Bromides and Chlorides. *ACS Catalysis* **2020**, *10* (11), 6030-6041.
- 25. Tomasi, J.; Mennucci, B.; Cammi, R., Quantum mechanical continuum solvation models. *Chem. Rev.* **2005**, *105*, 2999-3093.
- 26. Svanqvist, M.; Hansen, K., Non-jellium scaling of metal cluster ionization energies and electron affinities. *Eur. Phys. J. D* **2010**, *56* (2), 199-203.
- 27. Muzart, J., Palladium-catalyzed oxidation of primary and secondary alcohols. *Tetrahedron* **2003**, *59*, 5789-5816.
- 28. Deitrich, R.; Zimatkin, S.; Pronko, S., Oxidation of ethanol in the brain and its consequences. *Alcohol Res. Health* **2006**, *29*, 266-273.
- 29. Amatore, C.; Le Duc, G.; Jutand, A., Mechanism of Palladium-Catalyzed Suzuki-Miyaura Reactions: Multiple and Antagonistic Roles of Anionic "Bases" and Their Countercations. *Chem. Eur. J.* **2013**, *19* (31), 10082-10093.
- 30. Amatore, C.; Jutand, A.; Due, G. L., Kinetic Data for the Transmetalation/Reductive Elimination in Palladium-Catalyzed Suzuki-Miyaura Reactions: Unexpected Triple Role of Hydroxide Ions Used as Base. *Chem. Eur. J* **2011**, *17*, 2492-2503.

SYNOPSIS TOC

